

# Cascaded digital lattice Boltzmann automata for high Reynolds number flow

Martin Geier,\* Andreas Greiner, and Jan G. Korvink

*Lab for Simulation, Department of Microsystems Engineering (IMTEK), University of Freiburg,  
Georges-Köhler-Allee 103, 79110 Freiburg, Germany*

(Received 22 December 2005; revised manuscript received 24 February 2006; published 20 June 2006)

Lattice Boltzmann methods are of limited applicability for direct numerical simulation of turbulent flow due to instabilities in the zero viscosity limit. We observe that this is caused by an insufficient degree of Galilean invariance of the relaxation-type Lattice Boltzmann collision operator. The cascaded digital lattice Boltzmann automata described here, provides a method with which to achieve stable collision operators down to the limit of zero viscosity.

DOI: [10.1103/PhysRevE.73.066705](https://doi.org/10.1103/PhysRevE.73.066705)

PACS number(s): 47.11.Qr, 47.27.ek, 47.27.E-

## I. INTRODUCTION

Turbulent flow appears to be chaotic. It contains eddies of a large spectrum of sizes and hence a lot of information that is to be tracked when one tries to simulate turbulent flow on a digital computer. The dimensionless measure of turbulence is the Reynolds number  $Re = Lv\nu^{-1}$ , with the characteristic length of the system  $L$ , the velocity  $v$ , and the kinematic viscosity  $\nu$ . The number of computational nodes necessary to resolve three-dimensional turbulent flow scales as  $N = O(Re^{9/4}) = O((Lv)^{9/4}\nu^{-9/4})$  [1,2]. Obviously, the number of nodes could be reduced by letting  $\nu \rightarrow 0$ . This is, however, not trivial since most numerical discretization schemes tend to have a great amount of numerical dissipation. A notable exception is the lattice Boltzmann automaton (LBA), which has very little numerical dissipation. Its main drawback appears to be the property to become unstable for small viscosities. We identified insufficient Galilean invariance of the standard LBA as the source for this instabilities and present an improved LBA allowing us to lower viscosity by many orders of magnitude as compared to the original model.

## II. LATTICE BOLTZMANN METHOD

A LBA [3–7] is a set of nodes arranged on a Cartesian grid. The nodes are connected via links to a finite set of neighbors. Links are occupied by particles moving from one node to the next in the *streaming step*. (We shall restrict ourself to digital LBA with an integer amount of particles on every link. Digital LBA are free from roundoff errors [9].) After the streaming step, a *scattering step* follows in which all particles accumulated on a given node are rearranged, usually in a mass and momentum conserving manner.

Deriving the scattering operator from the Navier-Stokes equation does not provide enough constraints to fix all degrees of freedom. As a result, there is a range of scattering operators, all compatible with the Navier-Stokes equation. The most common ones are the single relaxation time (SRT) [10,11] and the multiple relaxation time (MRT) [14] operators. Both are based on a second-order approximation of the Maxwell-Boltzmann distribution to which the incoming state

of the node is relaxed either in a single step or in multiple steps. MRT is a refinement of the earliest LBA pioneered in matrix form [12,13]. MRT operators exploit the fact that the kinematic viscosity of LBA depends only on the relaxation constant of second-order moments  $\omega_{\alpha\beta}$ :

$$\tilde{\nu} = \frac{1}{3} \left( \frac{1}{\omega_{\alpha\beta}} - \frac{1}{2} \right), \quad (1)$$

where the viscosity  $\tilde{\nu}$  is given in units of  $\Delta l^2 / \Delta t$ , with  $\Delta l$  and  $\Delta t$  denoting the grid spacing and the time step, respectively. In order to increase  $Re$  we would like to choose  $\omega_{\alpha\beta}$  as close to 2 as possible.

The MRT operators perform better when compared to SRT because they allow for the choice of lower relaxation constants for the remaining nonhydrodynamic moments. However, neither the SRT nor the MRT is stable in the limit of  $\omega_{\alpha\beta}$  approaching 2. A new class of scattering operators based on transcendent entropic functionals has recently been suggested. Entropic lattice Boltzmann automata [15–17] enforce an  $H$ -theorem on the lattice and are hence unconditionally stable. That is achieved by modulating the relaxation time in dependence on local entropy, which effectively removes high frequencies from the flux fields. The method we propose does not remove any frequencies, but rather aims to deal with the highest frequencies with sufficient accuracy so that they do not compromise the overall stability.

## III. CASCADED DIGITAL SCATTERING OPERATOR

Cascaded digital lattice Boltzmann automata (CDLBA) aim at removing the kind of instabilities from the LBA that can be traced back to the insufficient degree of Galilean invariance. We identified three major reasons for the violation of Galilean invariance in the relaxation-type LBA:

(a) The equilibrium distribution is typically chosen to be Galilean invariant only up to second order in Mach number.

(b) Many implementations use insufficient finite velocity sets with 13, 15, or 19 speeds.

(c) The crosstalk among central moments during the relaxation is typically not accounted for.

The choice of an equilibrium distribution of second order in Mach number is linked to the large-wavelength assump-

\*Electronic address: [geier@imtek.de](mailto:geier@imtek.de)

tion underlying the idea that LBA was a discretization of the Navier-Stokes equation. The large-wavelength assumption is invalid since instabilities typically arise from small wavelength patterns. A given velocity set allows us to approximate the correct Maxwell-Boltzmann distribution up to a certain number of moments (the same number as the number of speeds). Without choosing all supported moments as being Galilean invariant, the equilibrium distributions are not uniquely determined. The remaining degrees of freedom are set to arbitrary values.

Popular velocity sets, such as 19 velocities in three dimensions, are insufficient to adjust different moments independently. The set of 19 velocities allows the particles to move along the coordinate axis and in the  $xy$ ,  $xz$ , and  $yz$  directions but not in the  $xyz$  directions. Hence, the trilinear moment  $\mu_{xyz}$  with respect to velocity cannot be chosen independently from other moments. This particular moment is not considered to be important in the long wavelength assumption. It becomes, however, very important when we consider short wavelength structures in the flow field. We might interpret the moment  $\mu_{xyz}$  as the advection of the moment  $\mu_{xy}$  in the  $z$  direction or the advection of  $\mu_{yz}$  in the  $x$  direction and so on. The moment  $\mu_{xy}$  is associated with the shear rate and is certainly important. Neglecting the moment  $\mu_{xyz}$  means that the advection of shear rate is neglected. This is invalid for flows with short wavelength features.

Transport parameters are associated with the relaxation rate of specific moments of the single-node particle distribution function. Since we consider the flow as being Galilean invariant it is understood that the relaxation rates correspond to central moments (moments displaced by the velocity). However, due to the fixed lattice, we are always relaxing raw moments (moments with respect to velocity zero). Central moments can be expressed as polynomials of all raw moments up to the same order as the central moment. Thus, central moments do not depend on raw moments of higher order. A central moment can always be relaxed by relaxing the corresponding raw moment. However, relaxing a raw moment implies a change in all higher central moments. This crosstalk is certainly a source of instability.

CDLBA solves all three problems. For athermal fluids, we choose the complete velocity set of unit speed particles [ $3^2=9$  in two (2D) and  $3^3=27$  in three dimensions (3D)]. These models have only 9 and 27 independent raw moments in two and three dimensions, respectively. We match the same number of central moments and achieve the corresponding order of Galilean invariance. In order to do this, we choose an orthogonal decomposition of the momentum distribution in terms of raw moments, as known from the multiple relaxation time LBA. Our aim is to relax central moments, but the decomposition allows us only to relax raw moments. We know that central moments of a certain order are polynomials of raw moments up to the same order. Starting with the lowest moment we can adjust the corresponding central moment by relaxing the raw moment toward its equilibrium (chosen from the Maxwell-Boltzmann distribution). This effects all subsequent (higher-order) central moments. However, this error is known analytically and can be compensated for by subtracting it from all higher-order moments

before relaxing them. There is no crosstalk from the relaxation of high-order raw moments to the lower-order central moments. The key is that we are able to process the scattering cascade in a single pass going from the lowest order moments towards the highest-order moments. This means that Galilean invariance is generalized for the CDLBA and extended to higher moments. It is not sufficient to only make the equilibria of nonconserved moments independent of conserved moments. All equilibria must also be independent of the state of all other moments. Knowing the exact value of the overall equilibrium is of little help since over-relaxation results in off-equilibrium state vectors. Because lower-order moments interfere with higher-order moments and since the lower-order moments are not in equilibrium after the collision, it is not possible to know the equilibria of all moments prior to collision. However, relaxing the moments order by order, beginning with the lowest and ending with the highest, and taking the post-collision values of all processed moments into account, resolves this issue.

#### IV. CDLB IN 2D

Here we derive the CDLBA in two dimensions. The nodal state vector of the D2Q9 (two dimensions, nine speeds) lattice is given as

$$\vec{s} = (r, nw, w, sw, s, se, e, ne, n)^T, \quad (2)$$

where  $r$  corresponds to the occupation number of the resting link while the other links are indicated by the cardinal direction they are pointing at, counterclockwise from northwest to north. In order to impose Galilean invariance constraints on the moments we have to find a mapping from configuration space to equivalent moment space. For the D2Q9 lattice this can be obtained with the following orthogonal transformation matrix:

$$K = \begin{bmatrix} 1 & 0 & 0 & -4 & 0 & 0 & 0 & 0 & 4 \\ 1 & -1 & 1 & 2 & 0 & 1 & -1 & 1 & 1 \\ 1 & -1 & 0 & -1 & 1 & 0 & 0 & -2 & -2 \\ 1 & -1 & -1 & 2 & 0 & -1 & 1 & 1 & 1 \\ 1 & 0 & -1 & -1 & -1 & 0 & -2 & 0 & -2 \\ 1 & 1 & -1 & 2 & 0 & 1 & 1 & -1 & 1 \\ 1 & 1 & 0 & -1 & 1 & 0 & 0 & 2 & -2 \\ 1 & 1 & 1 & 2 & 0 & -1 & -1 & -1 & 1 \\ 1 & 0 & 1 & -1 & -1 & 0 & 2 & 0 & -2 \end{bmatrix}, \quad (3)$$

$$K = [\vec{K}_0, \dots, \vec{K}_8]. \quad (4)$$

The vectors  $\vec{K}_i$  are chosen so that there is one for each moment.

The lowest moments correspond to the conserved quantities mass and momentum:

$$\rho = \vec{s} \cdot \vec{K}_0, \quad (5)$$

$$v_x = \vec{s} \cdot \vec{K}_1 \rho^{-1}, \quad (6)$$

$$v_y = \vec{s} \cdot \vec{K}_2 \rho^{-1}. \quad (7)$$

The relaxation time approximation assumes central moments to relax to fix points given by the equilibrium distribution function which is the Maxwell-Boltzmann distribution in the case of an ideal gas. We define central moments in 2D as

$$\kappa_{x^m y^n} = \sum_i s_i (c_{ix} - v_x)^m (c_{iy} - v_y)^n, \quad (8)$$

with  $c_{i\alpha}$  being the vector component of link  $i$  in direction  $\alpha$ . The central moments for the equilibrium distribution are constant. Odd moments vanish. Even moments are chosen from the Maxwell-Boltzmann distribution for an isothermal ideal gas:

$$\kappa_{xx}^{eq} = \kappa_{yy}^{eq} = \frac{1}{3} \rho, \quad (9)$$

$$\kappa_{xxyy}^{eq} = \frac{1}{9} \rho. \quad (10)$$

Transport coefficients such as viscosity are determined by the relaxation rate of specific central moments. Our aim is to adjust each central moment independently. A feasible solution is to solve a set of linear equations at each node in each time step. However, this cannot be done without introducing roundoff errors into the conserved quantities. Instead, we make use of the fact that central moments  $\kappa_{x^l y^m}$  can be expressed as polynomials of the raw moments up to the same order. With the central moments of the post-collision state known from the Maxwell-Boltzmann distribution, we can solve for the deviation of the raw moments from their equilibrium values. This has to be done step by step. We start with the set  $\{\kappa_{xx}, \kappa_{yy}\}$ :

$$\kappa_{xx}^{eq} = \sum_i s_i^p (c_{ix} - v_x)^2, \quad (11)$$

$$\kappa_{yy}^{eq} = \sum_i s_i^p (c_{iy} - v_y)^2, \quad (12)$$

where  $s_i^p$  are the components of the post-collision state vector:

$$\vec{s}^p = \vec{s} + K \cdot \vec{k}. \quad (13)$$

For the derivation we assume that the post-collision state was the equilibrium state. Later we drop this assumption. It is easily seen that  $\kappa_{xx}$  and  $\kappa_{yy}$  depend only on  $k_3$  and  $k_4$ . Solving this yields

$$k_3^{eq} = [\rho(v_x^2 + v_y^2) - e - n - s - w - 2(se + sw + ne + nw - \rho/3)]/12, \quad (14)$$

$$k_4^{eq} = [n + s - e - w + \rho(v_x^2 - v_y^2)]/4. \quad (15)$$

The actual values for  $k_3$  and  $k_4$  depend, via relaxation constants  $\omega_3$  and  $\omega_4$ , on the corresponding transport coefficients. In addition, we introduce a truncation operator ( $\lfloor \cdot \rfloor$ ) in order to obtain an integer state vector. Thus, we get

$$k_3 = \lfloor \omega_3 [\rho(v_x^2 + v_y^2) - e - n - s - w - 2(se + sw + ne + nw - \rho/3)]/12 \rfloor, \quad (16)$$

$$k_4 = \lfloor \omega_4 [n + s - e - w + \rho(v_x^2 - v_y^2)]/4 \rfloor. \quad (17)$$

The bilinear central moment  $\kappa_{xy}$  depends only on  $k_5$ . It can be obtained from

$$\kappa_{xy}^{eq} = \sum_i s_i^p (c_{ix} - v_x)(c_{iy} - v_y). \quad (18)$$

For  $k_5$ , we get

$$k_5 = \lfloor \omega_5 [(ne + sw - nw - se) - v_x v_y \rho]/4 \rfloor. \quad (19)$$

The moments we dealt with so far are those corresponding to the shear viscosity. It is the common tenet that the Galilean invariance and the relaxation constants of all further moments are of no particular interest since they do not effect the Navier-Stokes equation. By taking these moments into account, the derivation becomes more complicated because the next group of central moments depends on relaxation constants whose values we have already fixed. For adjusting  $\kappa_{xxy}$  and  $\kappa_{xyy}$ , we get

$$k_6^{eq} = (-\{[se + sw - ne - nw - 2v_x^2 v_y \rho + v_y(\rho - n - s - r)]/4 + v_x/2(ne - nw - se + sw)\} - v_y/2(-3k_3 - k_4) - 2v_x k_5), \quad (20)$$

$$k_7^{eq} = (-\{[sw + nw - se - ne - 2v_y^2 v_x \rho + v_x(\rho - w - e - r)]/4 + v_y(ne + sw - se - nw)/2\} - v_x/2(-3k_3 + k_4) - 2v_y k_5). \quad (21)$$

The equilibrium of the higher-order moments depend on the post-collision state. The values for  $k_3$ ,  $k_4$ , and  $k_5$  are already determined. However, it is important to note that if we add relaxation constants, we must not multiply them with the  $k_\alpha$  since they correspond to the post-collision state while the relaxation process goes from pre-collision to post-collision. Thus, we get

$$k_6 = \lfloor \omega_6 (-\{[se + sw - ne - nw - 2v_x^2 v_y \rho + v_y(\rho - n - s - r)]/4 + v_x/2(ne - nw - se + sw)\} - v_y/2(-3k_3 - k_4) - 2v_x k_5) \rfloor, \quad (22)$$

$$k_7 = \lfloor \omega_7 (-\{[sw + nw - se - ne - 2v_y^2 v_x \rho + v_x(\rho - w - e - r)]/4 + v_y(ne + sw - se - nw)/2\} - v_x/2(-3k_3 + k_4) - 2v_y k_5) \rfloor. \quad (23)$$

By the same argument, we obtain

$$\begin{aligned}
 k_8 = & [\omega_8(1/4\{\rho/9 - ne - nw - se - sw \\
 & + 2[v_x(ne - nw + se - sw) \\
 & + v_y(ne + nw - se - sw)] \\
 & + 4v_xv_y(nw - ne + se - sw) \\
 & - v_x^2(n + ne + nw + s + se + sw) \\
 & + v_y^2(3v_x^2\rho - e - ne - nw - se - sw - w)\}) \\
 & - 2k_3 - 2v_xk_7 - 2v_yk_6 + 4v_xv_yk_5 \\
 & - (3/2k_3 - k_4/2)(v_x^2 + v_y^2)], \quad (24)
 \end{aligned}$$

using

$$\kappa_{xyy}^{eq} = \sum_i s_i^p (c_{ix} - v_x)^2 (c_{iy} - v_y)^2. \quad (25)$$

The final scattering operation is then

$$\vec{s} \leftarrow \vec{s} + K \cdot \vec{k}. \quad (26)$$

For isotropic viscosity, we require  $\omega_4 = \omega_5 = \omega_{\alpha\beta}$ . The speed of sound is  $c_s = 1/\sqrt{3}$ . This model is typically stable for  $\omega_{\alpha\beta} = 2$  and all other relaxation parameters set to unity, meaning (theoretically) zero viscosity. It is, however, sensitive to violations of the Courant-Friedrichs-Lewy (CFL) condition [8]. Since sound propagation must be Galilean invariant and information must travel less than one lattice spacing per time step, the velocity must be smaller than  $v_{max} = 1 - c_s \approx 0.42[\Delta t/\Delta t]$ .

### V. CDLBA IN 3D

In 3D, 27 degrees of freedom are necessary in order to obtain an CDLBA that is stable for arbitrary low viscosities. On lattices with only 13, 15, or 19 links per node it is not possible to impose Galilean invariance on third-order moments. Hence, here is no convection of shear rate, which is fatal for short-wavelength turbulence. The D3Q27 scattering operators are presented in the Appendix.

### VI. RESULTS

In order to determine the lower viscosity bound of the CDLBA, we simulate the decay of a shear wave in a periodic box of dimensions  $30 \times 3 \times 3$  with different superimposed flow fields. The wave vector points along the long axis. We chose  $\omega_{\alpha\beta} = 2$  corresponding to  $\tilde{v} = 0$ . Turbulent behavior requires a finite but small amount of dissipation. It turns out that a positive rest viscosity remains at  $\omega_{\alpha\beta} = 2$ . It can be determined from the autocorrelation of the velocity field. The simulation domain is small; however, the outcome of the simulation is in fact independent of the size of the domain. The initial conditions differ only in the direction of the wave vector. The three layers of nodes along the short axis have identical initial conditions. Since the algorithm is deterministic and free from roundoff errors, the result of the scattering process is the same for all layers of nodes. Each layer is identical to both neighboring layers and stays so after streaming.

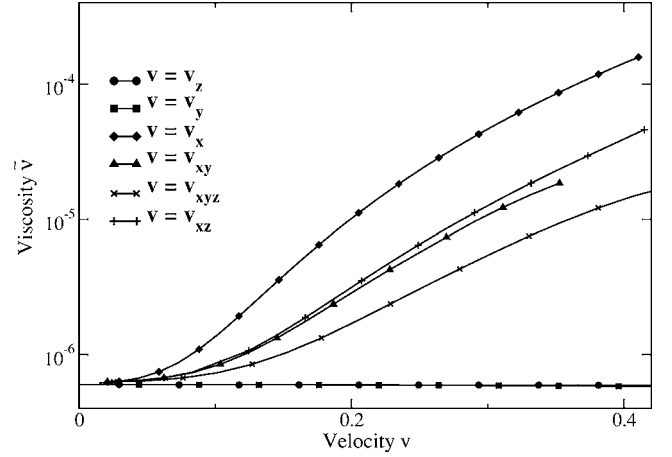


FIG. 1. Viscosity versus superimposed flow speed (both in lattice units) on a  $30 \times 3 \times 3$  D3Q27 lattice obtained from the decay of a shear wave with amplitude pointing in the  $y$  direction and a wave vector pointing in the  $x$  direction. The desired viscosity is zero ( $\omega_{\alpha\beta} = 2$ ). The superimposed flow fields point in the axial and diagonal directions.

On the D3Q27 lattice all third-order moments except the three longitudinal ones ( $\kappa_{\alpha\alpha\alpha}$ ) are made Galilean invariant. Superimposed transversal flow fields have no visible influence on the viscosity. However, flow fields in the longitudinal direction can increase the viscosity by more than two orders of magnitude in the stable range (see Fig. 1). The relevant stability criterion for turbulent flow is imposed by the transport of shear rate with the mean flow, which is a transverse effect. Most important is the fact that viscosity is always found to be positive, since only negative viscosity compromises stability, while positive viscosity artifacts reduce only the accuracy. Errors in viscosity are small for flow speeds  $v < 0.1$  in lattice units, which is reasonable considering the CFL condition. The undesired numerical viscosity is independent of  $\omega_{\alpha\beta}$  and becomes negligible for finite Reynolds numbers. We find a remaining rest viscosity of  $\tilde{v} \approx 10^{-6}$ . This lower viscosity limit is found to depend on the numerical precision of the applied data type. Our current implementation uses 32-bit signed integers to represent link data. This imposes an upper bound on the number of particles allowed on a node [18]. Increasing the average number of particles per node ( $\tilde{\rho}$ ) improves numerical precision and leaves the physics unchanged. The lowest attainable viscosity for  $\omega_{\alpha\beta} = 2$  was measured to depend on the number of particles per node as  $\tilde{v} \sim 1/\tilde{\rho}$ . No saturation effect was observed in the available range of 32-bit integers. This indicates that highly turbulent flows can only be simulated with high precision data types. More precisely speaking, we observe exponential growth of the attainable Reynolds number as a function of the number of bits used for the data type of the occupation number.

Showing that CDLBA holds its promise for actual simulations of turbulent flow is not straightforward since no analytical solutions are known for fully developed turbulent flow. The plausibility of the result can only be checked indirectly, for example by measuring the Kolmogorov exponent

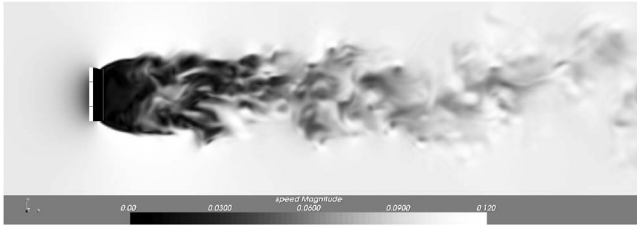


FIG. 2. Turbulent velocity field in the wake of a rectangular obstacle at a nominal Reynolds number  $Re=1\,400\,000$ . The computational mesh has  $120 \times 120 \times 400$  nodes and the Mach number is  $Ma=0.168$ . The grid resolution is too coarse to host the nominal Reynolds number. Yet, the lack of the unresolved eddies does not ruin the resolved scales. The picture shows a cut through the central plane of the simulation domain.

of the spectral distribution of kinetic energy. Theory [1,19] predicts an energy spectrum  $E \sim k^{-5/3}$  for turbulent flow irrespective of its origin. Here  $k$  denotes the spatial wave number. We simulate the flow around a rectangular plate ( $20 \times 30$  nodes wide) at  $\nu=2 \times 10^{-6}$  and  $v=0.097$  corresponding to a Mach number  $Ma=0.168$ . The mesh has  $120 \times 120 \times 400$  nodes and the simulation is run for a duration of 18 160 time steps. The resulting Reynolds number is  $Re=1\,400\,000$  and the flow condition must be considered fully turbulent while the grid resolution is insufficient to represent the full spectrum of excited wave numbers. (That is to say, we run an under-resolved simulation without resorting to turbulence modeling, filtering, or entropic stabilization.) Pressure boundary conditions are applied in the  $x$  direction. Boundary conditions in the  $y$  and  $z$  directions are periodic. The obstacle is implemented with simple bounce back boundary conditions. Because CDLBA is fully deterministic and free from roundoff errors it is necessary to add a small random perturbation to the initial conditions in order to obtain the break in symmetry necessary to start turbulent behavior. A cut through the velocity field is presented in Fig. 2. Figure 3 shows the one-dimensional energy spectrum mea-

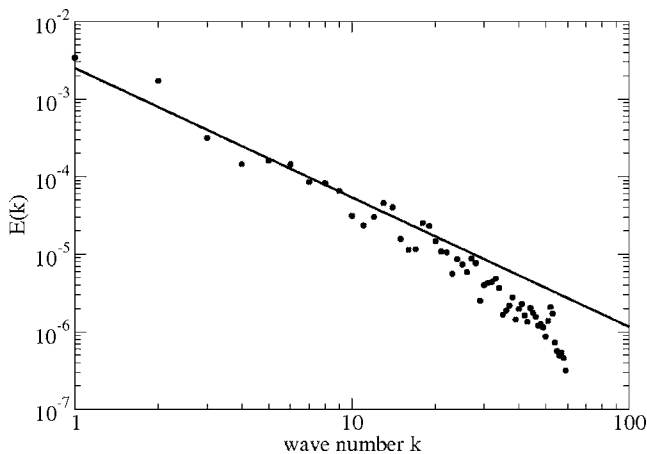


FIG. 3. One-dimensional energy spectrum in the wake of the flow behind an rectangular obstacle (Fig. 2) using reduced units. The line is a guide to the eye indicating the  $k^{-5/3}$  power law of the Kolmogorov spectrum.

sured perpendicular to the flow direction in the wake of the obstacle. The energy values are averaged over 5/12 of the simulation domain. Measuring starts 40 node spacings behind the obstacle. We recognize agreement with the  $E \sim k^{-5/3}$  law as indicated by the line. However, more simulations would be necessary to obtain enough data for a statistical analysis.

### VII. CONCLUSION

We pointed out that the common derivation of LBA scattering operators fail to determine all degrees of freedom and leave some choice for remaining high-order moments. Complete Galilean invariance requires all considered central moments to be independent of velocity and all other central moments. Crosstalk between different central moments due to the derivation from velocity zero is not accounted for in the original relaxation-type LBA. Since analytic expressions for the crosstalk are known, it is possible to compensate crosstalk exactly. Equipped with this fact, there are sufficient constraints to determine the formerly arbitrary degrees of freedom. The resulting relaxation operators are noncommuting, but they provide a natural ordering of their execution allowing to adjust all considered moments in a single pass. The method is completely explicit. It makes use of neither transcendental stabilization functionals nor root finding. We have not used the assumption of a local  $H$ -theorem and entropy was not considered in the derivation. The instabilities of the LBA in the high  $Re$  limit are drastically reduced with the CDLBA. The actual lowest attainable viscosity depends exponentially on the width of the data type for link occupation numbers. Using integers might seem to be unnecessarily restrictive when compared with the flexibility of floating point numbers. However, when considering the low Mach number approximation, we see that the occupation numbers (particles per link) must all be of the same order of magnitude. Integers have more available digits for a given number of bits and computational results based only on integers are valid up to the least significant bit since no roundoff errors occur. Using floating point data types for the occupation numbers would not provide any benefit. Velocity, density, and relaxation constants have to be floating point numbers, of course. In contrast to entropic LBA and turbulence modeling, CDLBA neither make use of viscosity modulation nor of low-pass filtering. Whereas other methods try to eliminate high frequencies, CDLBA treat them accurately without compromising the accuracy for low frequencies. The objective of CDLBA is to capture physically correct behavior for the shortest wavelength fitting on the computational grid. We see this as the correct methodology to achieve the decoupling of the resolved and the unresolved scales in turbulent fluidic simulations. However, we have to admit that the model, as presented here, might overestimate the role of Galilean invariance especially in the high-order moments. Galilean invariance of fourth and sixth order is obtained only with excessive numerical overhead while the actual corrections are so small that it seems unlikely that they have any measurable influence on the stability and accuracy of the method.

**ACKNOWLEDGMENTS**

Partial funding of the project by the German Ministry of Science and Education BMBF under the project SIMOD and by the German Science Foundation under project TPA4 of SFB499 is gratefully acknowledged.

**APPENDIX: 3D MODEL**

The derivation of the D3Q27 model is in essence the same as for the D2Q9 model. However, the requirement of 27 degrees of freedom with up to order six polynomials as equilibrium functions makes the calculation a lengthy task. In order to write down the transformation matrix we use Kronecker deltas and the usual summation conventions:

$$\delta_\alpha = \delta_w + \delta_e,$$

$$\delta_\beta = \delta_n + \delta_s,$$

$$\delta_\gamma = \delta_f + \delta_b.$$

Here,  $f$  and  $b$  denote front and back, respectively. The matrix then looks as follows:

$$K = [\vec{K}_0, \dots, \vec{K}_{26}],$$

$$\vec{K}_0 = \delta_0 + \delta_\alpha + \delta_\beta + \delta_\gamma + \delta_{\alpha\beta} + \delta_{\alpha\gamma} + \delta_{\beta\gamma} + \delta_{\alpha\beta\gamma},$$

$$\vec{K}_1 = \delta_e + \delta_{e\beta} + \delta_{e\gamma} + \delta_{e\beta\gamma} - \delta_w - \delta_{w\beta} - \delta_{w\gamma} - \delta_{w\beta\gamma},$$

$$\vec{K}_2 = \delta_n + \delta_{an} + \delta_{n\gamma} + \delta_{an\gamma} - \delta_s - \delta_{as} - \delta_{s\gamma} - \delta_{as\gamma},$$

$$\vec{K}_3 = \delta_f + \delta_{\alpha f} + \delta_{\beta f} + \delta_{\alpha\beta f} - \delta_b - \delta_{\alpha b} - \delta_{\beta b} - \delta_{\alpha\beta b},$$

$$\vec{K}_4 = \delta_{wn} - \delta_{ws} + \delta_{es} - \delta_{en},$$

$$\vec{K}_5 = \delta_{wf} - \delta_{wb} + \delta_{eb} - \delta_{ef},$$

$$\vec{K}_6 = \delta_{nb} - \delta_{nf} + \delta_{sf} - \delta_{sb},$$

$$\vec{K}_7 = \delta_\alpha - \delta_\beta,$$

$$\vec{K}_8 = \delta_\alpha - \delta_\gamma,$$

$$\vec{K}_9 = -30\delta_0 + 8(\delta_{\alpha\beta} + \delta_{\alpha\gamma} + \delta_{\beta\gamma}) - 11(\delta_\alpha + \delta_\beta + \delta_\gamma),$$

$$\vec{K}_{10} = \delta_{e\beta} + \delta_{e\gamma} - \delta_{w\beta} - \delta_{w\gamma} + 4(\delta_w - \delta_e),$$

$$\vec{K}_{11} = \delta_{an} + \delta_{n\gamma} - \delta_{as} - \delta_{s\gamma} + 4(\delta_s - \delta_n),$$

$$\vec{K}_{12} = \delta_{\alpha f} + \delta_{\beta f} - \delta_{\alpha b} - \delta_{\beta b} + 4(\delta_b - \delta_f),$$

$$\vec{K}_{13} = \delta_{w\gamma} - \delta_{w\beta} + \delta_{e\beta} - \delta_{e\gamma},$$

$$\vec{K}_{14} = \delta_{n\gamma} - \delta_{an} + \delta_{as} - \delta_{s\gamma},$$

$$\vec{K}_{15} = \delta_{\alpha f} - \delta_{\beta f} + \delta_{\beta b} - \delta_{\alpha b},$$

$$\vec{K}_{16} = \delta_{wnb} - \delta_{enb} + \delta_{enf} - \delta_{wnf} - \delta_{wsb} + \delta_{esb} - \delta_{esf} + \delta_{wsf},$$

$$\vec{K}_{17} = 12\delta_0 + \delta_{\alpha\beta} + \delta_{\alpha\gamma} + \delta_{\beta\gamma} - 4(\delta_\alpha + \delta_\beta + \delta_\gamma),$$

$$\vec{K}_{18} = \delta_{\alpha\beta} - \delta_{\beta\gamma} + 2(\delta_\gamma - \delta_\alpha),$$

$$\vec{K}_{19} = \delta_{\alpha\beta} - \delta_{\alpha\gamma} + 2(\delta_\gamma - \delta_\beta),$$

$$\vec{K}_{20} = 2(\delta_{sf} + \delta_{nb} - \delta_{nf} - \delta_{sb}) - \delta_{anb} - \delta_{asf} + \delta_{asb} + \delta_{anf},$$

$$\vec{K}_{21} = 2(\delta_{wf} + \delta_{eb} - \delta_{wb} - \delta_{ef}) - \delta_{w\beta f} - \delta_{e\beta b} + \delta_{w\beta b} + \delta_{e\beta f},$$

$$\vec{K}_{22} = 2(\delta_{nw} + \delta_{se} - \delta_{ne} - \delta_{sw}) - \delta_{nw\gamma} - \delta_{se\gamma} + \delta_{ne\gamma} + \delta_{sw\gamma},$$

$$\vec{K}_{23} = 2(\delta_{w\beta} + \delta_{w\gamma} - \delta_{e\beta} - \delta_{e\gamma}) + 4(\delta_e - \delta_w) - \delta_{w\beta\gamma} + \delta_{e\beta\gamma},$$

$$\vec{K}_{24} = 2(\delta_{as} + \delta_{s\gamma} - \delta_{an} - \delta_{an}) + 4(\delta_n - \delta_s) - \delta_{as\gamma} + \delta_{an\gamma},$$

$$\vec{K}_{25} = 2(\delta_{ab} + \delta_{\beta b} - \delta_{\alpha f} - \delta_{\beta f}) + 4(\delta_f - \delta_b) - \delta_{\alpha\beta b} - \delta_{\alpha\beta f},$$

$$\vec{K}_{26} = -8\delta_0 + 4(\delta_\alpha + \delta_\beta + \delta_\gamma) - 2(\delta_{\alpha\beta} + \delta_{\alpha\gamma} + \delta_{\beta\gamma}) + \delta_{\beta\gamma}.$$

Again, we have

$$\rho = \vec{s} \cdot \vec{K}_0,$$

$$v_x = \frac{\vec{s} \cdot \vec{K}_1}{\rho},$$

$$v_y = \frac{\vec{s} \cdot \vec{K}_2}{\rho},$$

$$v_z = \frac{\vec{s} \cdot \vec{K}_3}{\rho}.$$

The central moments are taken from the Maxwell-Boltzmann distribution for  $c_s = 1/\sqrt{3}$ :

$$\kappa_{xx}^{eq} = \frac{1}{3}\rho,$$

$$\kappa_{xxyy}^{eq} = \frac{1}{9}\rho,$$

$$\kappa_{xxyyzz}^{eq} = \frac{1}{27}\rho.$$

All odd moments vanish and the others follow from symmetry. The equilibrium functions for the moments and the corresponding over-relaxed vector  $\vec{k}$  can be derived in the same way one does for the D2Q9 lattice:

$$k_0 = 0, \quad k_1 = 0, \quad k_2 = 0, \quad k_3 = 0,$$

$$k_4 = [\omega_4(ne + neb + nef - nw - nwb - nwf - se - seb - sef + sw + swb + swf - v_x v_y \rho)/4],$$

$$k_5 = [\omega_5(ef - eb - neb + nef + nwb - nwf - seb + sef + swb - swf + wb - wf - v_x v_z \rho)/4],$$

$$k_6 = [\omega_6(sb - neb + nef + nf - nwb + nwf + nb + seb - sef - sf + swb - swf - v_z v_y \rho)/4],$$

$$k_7 = [\omega_7[-b - e - f + nb + ne + nf + nw + sb + se + sf + sw - w + 2(-eb - ef + n + s - wb - wf) + \rho(v_z^2 - 2v_y^2 + v_x^2)]/6],$$

$$k_8 = [\omega_8[-e + eb + ef - n + nb + nf - s + sb + sf - w + wb + wf + 2(b + f - ne - nw - se - sw) + \rho(v_x^2 + v_y^2 - 2v_z^2)]/6],$$

$$k_9 = [\omega_9[-b - e - f - n - s - w + 2(-eb - ef - nb - ne - nf - nw - sb - se - sf - sw - wb - wf) + 3(-neb - nef - nwb - nwf - seb - sef - swb - swf) + \rho(1 + v_y^2 + v_z^2 + v_x^2)]/126],$$

$$k_{10} = [\omega_{10}(nw + sw + wf + wb - eb - ef - ne - se + v_x\{b + eb + ef + 84k_9/\omega_{10} + f + n + ne + nw + s + se + sw + wb + wf + 2[nb + neb + nef + nf + nwb + nwf + sb + seb + sef + sf + swb + swf - (k_7 + k_8)/\omega_{10}]\} + 2[-neb - nef + nwb + nwf - seb - sef + swb + swf - v_y XY(\omega_{10}) - v_z XZ(\omega_{10})] - 2v_x \rho(v_y^2 + v_z^2))/8],$$

$$k_{11} = [\omega_{11}\{sb + sf + se + sw - nw - ne - nf - nb + v_y[b + e + 84k_9/\omega_{11} + f + nb + ne + nf + nw + sb + se + sf + sw + w + 2(eb + ef + neb + nef + nwb + nwf + seb + sef + swb + swf + wb + wf + k_7/\omega_{11})] + 2[-neb - nef - nwb - nwf + seb + sef + swb + swf - v_x XY(\omega_{11}) - v_z YZ(\omega_{11})] - 2v_y \rho(v_x^2 + v_z^2)\}/8],$$

$$k_{12} = [\omega_{12}\{eb + nb + sb + wb - ef - nf - sf - wf + v_z[e + eb + ef + n + nb + nf + s + sb + sf + w + wb + wf + 84k_9/\omega_{12} + 2(ne + neb + nef + nw + nwb + nwf + se + seb + sef + sw + swb + swf + k_8/\omega_{12})] + 2[-nef + neb + nwb - nwf + seb - sef + swb - swf - v_x XZ(\omega_{12}) - v_y YZ(\omega_{12})] - 2v_z \rho(v_x^2 + v_y^2)\}/8],$$

$$k_{13} = [\omega_{13}\{eb + ef - ne + nw - se + sw - wb - wf + v_x[-b - eb - ef - f + n + ne + nw + s + se + sw - wb - wf + 2(k_8 - k_7)/\omega_{13}]\}/8 + [v_z XZ(\omega_{13}) - v_y XY(\omega_{13}) + \rho v_x(v_z^2 - v_y^2)]/4],$$

$$k_{14} = [\omega_{14}\{ne - nb - nf + nw + sb - se + sf - sw + v_y[-e + b + f + nb - ne + nf - nw + sb - se + sf - sw - w + 2(-k_7 - 2k_8)/\omega_{14}]\}/8 + [v_x XY(\omega_{14}) - v_z YZ(\omega_{14}) + \rho v_y(v_x^2 - v_z^2)]/4],$$

$$k_{15} = [\omega_{15}\{eb - ef - nb + nf - sb + sf + wb - wf + v_z[e + eb + ef - n - nb - nf - s - sb - sf + w + wb + wf + 2(k_8 + 2k_7)/\omega_{15}]\}/8 + [v_y YZ(\omega_{15}) - v_x XZ(\omega_{15}) + \rho v_z(v_y^2 - v_x^2)]/4],$$

$$k_{16} = [\omega_{16}[neb - nef - nwb + nwf - seb + sef + swb - swf - v_x YZ(\omega_{16}) - v_y XZ(\omega_{16}) - v_z XY(\omega_{16}) - 2\rho v_x v_y v_z]/8],$$

$$k_{17} = [\omega_{17}[(\rho/3 - 96k_9/\omega_{17} - eb - ef - nb - ne - nf - nw - sb - se - sf - sw - wb - wf - 3(nwf + nwb + nef + neb + swf + swb + sef + seb) + 2[v_x X(\omega_{17}) + v_y Y(\omega_{17}) + v_z Z(\omega_{17})] + v_x^2\{-84k_9/\omega_{17} - b - eb - ef - f - n - ne - nw - s - se - sw - wb - wf + 2[(k_7 + k_8)/\omega_{17} - nb - neb - nef - nf - nwb - nwf - sb - seb - sef - sf - swb - swf]\} + v_y^2[-84k_9/\omega_{17} - b - e - f - nb - ne - nf - nw - sb - se - sf - sw - w + 2(-k_7/\omega_{17} - eb - ef - neb - nef - nwb - nwf - seb - sef - swb - swf - wb - wf)] + v_z^2[-84k_9/\omega_{17} - e - eb - ef - n - nb - nf - s - sb - sf - w - wb - wf + 2(-k_8/\omega_{17} - ne - neb - nef - nw - nwb - nwf - se - seb - sef - sw - swb - swf)] + 4[v_x v_y XY(\omega_{17}) + v_x v_z XZ(\omega_{17}) + v_y v_z YZ(\omega_{17})] + 3\rho(v_x^2 v_y^2 + v_x^2 v_z^2 + v_y^2 v_z^2)]/12],$$

$$k_{18} = [\omega_{18}[-eb - ef - ne - nw - se - sw - wb - wf + 2(nb + nf + sb + sf + v_x X(\omega_{18}) + v_y \{ne - neb - nef + nw - nwb - nwf - se + seb + sef - sw + swb + swf + 2[sf + sb - nb - nf - (2k_{11} + 6k_{14})/\omega_{18}]\} + v_z \{ef - eb + neb - nef + nwb - nwf + seb - sef + swb - swf - wb + wf + 2[nb - nf + sb - sf - (2k_{12} - 6k_{15})/\omega_{18}]\}) + v_x^2 \{-b - eb - ef - f - n - ne - nw - s - se - sw - wb - wf - 84k_9/\omega_{18} - 2[nb + neb + nef + nf + nwb + nwf + sb + seb + sef + sf + swb + swf - (k_7 + k_8)/\omega_{18}]\} + v_y^2 \{eb - e + ef - ne + neb + nef - nw + nwb + nwf - se + seb + sef - sw + swb + swf - w + wb + wf + 42k_9/\omega_{18} + 2[b + f + nb + nf + sb + sf - (k_7 + 3k_8)/\omega_{18}]\} + v_z^2 \{ne - e - eb - ef + neb + nef + nw + nwb + nwf + se + seb + sef + sw + swb + swf - w - wb - wf + 42k_9/\omega_{18} + 2[n + nb + nf + s + sb + sf - (k_8 + 3k_7)/\omega_{18}]\} + 4\{v_x[v_y XY(\omega_{18}) + v_z XZ(\omega_{18})]\} - 8v_x v_y v_z YZ(\omega_{18}) + [-6v_x^2 v_z^2 + 3v_x^2(v_y^2 + v_z^2)]\rho]/12],$$

$$k_{19} = [\omega_{19}[-nb - ne - nf - nw - sb - se - sf - sw + 2(eb + ef + wb + wf + v_x \{ne - neb - nef - nw + nwb + nwf + se - seb - sef - sw + swb + swf + 2[wb + wf - eb - ef - (2k_{10} - 6k_{13})/\omega_{19}]\} + v_y Y(\omega_{19}) + v_z \{nf - nb + neb - nef + nwb - nwf - sb + seb - sef + sf + swb - swf + 2[eb - ef + wb - wf - (2k_{12} + 6k_{15})/\omega_{19}]\}) + v_x^2 \{nb - n - ne + neb + nef + nf - nw + nwb + nwf - s + sb - se + seb + sef + sf - sw + swb + swf + 42k_9/\omega_{19} + 2[b + eb + ef + f + wb + wf + (k_7 - 2k_8)/\omega_{19}]\} - v_y^2 \{b + e + f + nb + ne + nf + nw + sb + se + sf + sw + w + 84k_9/\omega_{19} + 2(eb + ef + neb + nef + nwb + nwf + seb + sef + swb + swf + wb + wf + k_7/\omega_{19})\} + v_z^2 \{ne - n - nb + neb + nef - nf + nw + nwb + nwf - s - sb + se + seb + sef - sf + sw + swb + swf + 42k_9/\omega_{19} + 2[e + eb + ef + w + wb + wf + (3k_7 + 2k_8)/\omega_{19}]\} + 4v_y[v_x XY(\omega_{19}) + v_z YZ(\omega_{19})] - 8v_x v_z XZ(\omega_{19}) + [-6v_x^2 v_z^2 + 3(v_x^2 + v_z^2)v_y^2]\rho]/12],$$

$$k_{20} = [\omega_{20}\{neb - nef + nwb - nwf - seb + sef - swb + swf + v_y Z_P(\omega_{20}) + v_z Y_N(\omega_{20}) + 2v_x[XYZ(\omega_{20}) + v_y XZ(\omega_{20}) + v_z XY(\omega_{20})] + v_x^2 YZ(\omega_{20}) + v_y v_z EPa(\omega_{20}) + \rho 3v_x^2 v_y v_z\}/8],$$

$$k_{21} = [\omega_{21}\{neb - nef - nwb + nwf + seb - sef - swb + swf + v_x Y_N(\omega_{21}) + v_z X_P(\omega_{21}) + 2v_y[XYZ(\omega_{21}) + v_x YZ(\omega_{21}) + v_z XY(\omega_{21})] + v_x^2 XZ(\omega_{21}) + v_x v_z EPc(\omega_{21}) + \rho 3v_y^2 v_x v_z\}/8],$$

$$k_{22} = [\omega_{22}\{nwb - neb - nef + nwf + seb + sef - swb - swf + v_x Y_P(\omega_{22}) + v_y X_N(\omega_{22}) + 2v_z[XYZ(\omega_{22}) + v_y XZ(\omega_{22}) + v_x YZ(\omega_{22})] + v_x^2 XY(\omega_{22}) + v_x v_y EPb(\omega_{22}) + \rho 3v_z^2 v_x v_y\}/8],$$

$$k_{23} = [\omega_{23}\{nwb - neb - nef + nwf - seb - sef + swb + swf - v_x A(\omega_{23}) - 2[v_y UZ(\omega_{23}) + v_z UY(\omega_{23})] - v_y^2 X_N(\omega_{23}) - v_z^2 X_P(\omega_{23}) + 2v_x[-v_y Y_P(\omega_{23}) - v_z Z_N(\omega_{23})] - 4v_y v_z[XYZ(\omega_{23}) + v_x YZ(\omega_{23})] - v_x[v_z^2 EPc(\omega_{23}) + v_y^2 EPb(\omega_{23})] - 2[v_y^2 v_z XZ(\omega_{23}) + v_x v_z^2 XY(\omega_{23})] - 4v_x v_y^2 v_z^2 \rho\}/8],$$

$$k_{24} = [\omega_{24}\{seb - neb - nef - nwb - nwf + sef + swb + swf - v_y C(\omega_{24}) - 2[v_x UZ(\omega_{24}) + v_z UX(\omega_{24})] - v_x^2 Y_P(\omega_{24}) - v_z^2 Y_N(\omega_{24}) + 2v_y[-v_x X_N(\omega_{24}) - v_z Z_P(\omega_{24})] - 4v_x v_z[XYZ(\omega_{24}) + v_y XZ(\omega_{24})] - v_y[v_x^2 EPb(\omega_{24}) + v_z^2 EPa(\omega_{24})] - 2[v_x^2 v_z YZ(\omega_{24}) + v_x v_z^2 XY(\omega_{24})] - 4v_x v_y^2 v_z^2 \rho\}/8],$$

$$k_{25} = [\omega_{25}\{neb - nef + nwb - nwf + seb - sef + swb - swf - v_z CA(\omega_{25}) - 2[v_x UY(\omega_{25}) + v_y UX(\omega_{25})] - v_x^2 Z_N(\omega_{25}) - v_y^2 Z_P(\omega_{25}) + 2v_z[-v_x X_P(\omega_{25}) - v_y Y_N(\omega_{25})] - 4v_x v_y[XYZ(\omega_{25}) + v_z XY(\omega_{25})] - v_z[v_x^2 EPc(\omega_{25}) + v_y^2 EPa(\omega_{25})] - 2[v_x^2 v_y YZ(\omega_{25}) + v_x v_y^2 XZ(\omega_{25})] - 4v_x^2 v_y^2 v_z \rho\}/8],$$

$$k_{26} = [\omega_{26}\{\rho/27 - neb - nef - nwb - nwf - seb - sef - swb - swf + 2[v_x(neb + nef - nwb - nwf + seb + sef - swb - swf + 8k_{23}/\omega_{26}) + v_y(neb + nef + nwb + nwf - seb - sef - swb - swf + 8k_{24}/\omega_{26}) + v_z(-neb + nef - nwb + nwf - seb + sef - swb + swf + 8k_{25}/\omega_{26})] + v_x^2 A(\omega_{26}) + v_y^2 C(\omega_{26}) + v_z^2 CA(\omega_{26}) + 4[v_x v_y UZ(\omega_{26}) + v_x v_z UY(\omega_{26}) + v_y v_z UX(\omega_{26})] + 2[v_x^2 v_y Y_P(\omega_{26}) + v_x^2 v_z Z_N(\omega_{26}) + v_y^2 v_z Z_P(\omega_{26}) + v_x v_y^2 X_N(\omega_{26}) + v_x v_z^2 X_P(\omega_{26}) + v_z^2 v_y Y_N(\omega_{26})] + 8v_x v_y v_z XYZ(\omega_{26}) + v_x^2 v_z^2 EPc(\omega_{26}) + v_x^2 v_y^2 EPb(\omega_{26}) + v_y^2 v_z^2 EPa(\omega_{26}) + 4v_x v_y v_z[v_z XY(\omega_{26}) + v_y XZ(\omega_{26}) + v_x YZ(\omega_{26})] + 5\rho v_x^2 v_y^2 v_z^2\}/8],$$

In the above we have used the following substitutions:

$$XY(\omega) = -ne - neb - nef + nw + nwb + nwf + se + seb + sef - sw - swb - swf + 4k_4/\omega,$$

$$XZ(\omega) = eb - ef + neb - nef - nwb + nwf + seb - sef - swb + swf - wb + wf + 4k_5/\omega,$$

$$YZ(\omega) = nb + neb - nef - nf + nwb - nwf - sb - seb + sef + sf - swb + swf + 4k_6/\omega,$$

$$X(\omega) = eb + ef + ne - nw + se - sw - wb - wf + 2(neb + nef - nwb - nwf + seb + sef - swb - swf) + 8k_{10}/\omega,$$

$$Y(\omega) = nb + ne + nf + nw - sb - se - sf - sw + 2(neb + nef + nwb + nwf - seb - sef - swb - swf) + 8k_{11}/\omega,$$

$$Z(\omega) = ef - eb - nb + nf - sb + sf - wb + wf + 2(nef - neb - nwb + nwf - seb + sef - swb + swf) + 8k_{12}/\omega,$$

$$X_N(\omega) = eb + ef + neb + nef - nwb - nwf + seb + sef - swb - swf - wb - wf + 4(k_{10} - k_{13})/\omega,$$

$$X_P(\omega) = ne + neb + nef - nw - nwb - nwf + se + seb + sef - sw - swb - swf + 4(k_{10} + k_{13})/\omega,$$

$$Y_N(\omega) = ne + neb + nef + nw + nwb + nwf - se - seb - sef - sw - swb - swf + 4(k_{11} - k_{14})/\omega,$$

$$Y_P(\omega) = nb + neb + nef + nf + nwb + nwf - sb - seb - sef - sf - swb - swf + 4(k_{11} + k_{14})/\omega,$$

$$Z_N(\omega) = nef - nb - neb + nf - nwb + nwf - sb - seb + sef + sf - swb + swf + 4(k_{12} - k_{15})/\omega,$$

$$Z_P(\omega) = nef - eb + ef - neb - nwb + nwf - seb + sef - swb + swf - wb + wf + 4(k_{12} + k_{15})/\omega,$$

$$XYZ(\omega) = -neb + nef + nwb - nwf + seb - sef - swb + swf + 8k_{16}/\omega,$$

$$EPa(\omega) = -42k_9/\omega - e - eb - ef - ne - neb - nef - nw - nwb - nwf - se - seb - sef - sw - swb - swf - w - wb - wf - 2(k_7 + k_8)/\omega,$$

$$EPb(\omega) = -42k_9/\omega - b - eb - ef - f - nb - neb - nef - nf - nwb - nwf - sb - seb - sef - sf - swb - swf - wb - wf + 2k_8/\omega,$$

$$EPc(\omega) = -42k_9/\omega - n - nb - ne - neb - nef - nf - nw - nwb - nwf - s - sb - se - seb - sef - sf - sw - swb - swf + 2k_7/\omega,$$

$$A(\omega) = (4k_{18} - 32k_9)/\omega - nb - neb - nef - nf - nwb - nwf - 4k_{17}/\omega - sb - seb - sef - sf - swb - swf,$$

$$C(\omega) = (4(k_{19} - k_{17}) - eb - ef - 32k_9)/\omega - neb - nef - nwb - nwf - seb - sef - swb - swf - wb - wf,$$

$$CA(\omega) = [-4(k_{18} + k_{19} + k_{17}) - 32k_9]/\omega - ne - neb - nef - nw - nwb - nwf - se - seb - sef - sw - swb - swf,$$

$$UZ(\omega) = nwb - neb - nef + nwf + seb + sef - swb - swf - 8k_{22}/\omega,$$

$$UY(\omega) = neb - nef - nwb + nwf + seb - sef - swb + swf - 8k_{21}/\omega,$$

$$UX(\omega) = neb - nef + nwb - nwf - seb + sef - swb + swf - 8k_{20}/\omega.$$

The moments have been arranged so that  $k_i=f(k_j)$  and  $k_j \neq f(k_i)$  for  $i > j$ . The relaxation constants for an isotropic shear viscosity are  $\omega_{\alpha\beta}=\omega_4=\omega_5=\omega_6=\omega_7=\omega_8$ . The equations can be simplified when other relaxation constants are set to one as has been done for the simulations presented in this paper.

- [1] U. Frisch, *Turbulence* (Cambridge University Press, Cambridge, UK, 1995).
- [2] K. R. Sreenivasan, *Rev. Mod. Phys.* **71**, S383 (1999).
- [3] R. Benzi, S. Succi, and M. Vergassola, *Phys. Rep.* **222**, 145 (1992).
- [4] S. Chen and G. Doolen, *Annu. Rev. Fluid Mech.* **30**, 329 (1998).
- [5] S. Succi, *The Lattice Boltzmann Equation* (Oxford University Press, New York, 2001).
- [6] U. Frisch, B. Hasslacher, and Y. Pomeau, *Phys. Rev. Lett.* **56**, 1505 (1986).
- [7] A. Ducan, M. Jason, and A. Michael, *Phys. Fluids* **17**, 100609 (2005).
- [8] R. Courant, K. Friedrichs, H. Lewy, *IBM J. Res. Dev.* **11**(2), 215 (1967).
- [9] H. Chen, C. Teixeira and K. Molvig, *Int. J. Mod. Phys. C* **8**(4), 675 (1997).
- [10] D. A. Wolf-Gladrow, *Lattice Gas Cellular Automata and Lattice Boltzmann Models: An Introduction* (Springer, Berlin, 2000).
- [11] P. Bhatnagar, E. Gross, and M. Krook, *Phys. Rev.* **94**, 511 (1954).
- [12] F. Higuera and J. Jimenez, *Europhys. Lett.* **9**, 663 (1989).
- [13] F. Higuera, S. Succi, and R. Benzi, *Europhys. Lett.* **9**, 345 (1989).
- [14] D. d’Humières, I. Ginzburg, M. Krafczyk, P. Lallemand, and L.-S. Lou, *Philos. Trans. R. Soc. London, Ser. A* **360**, 437 (2002).
- [15] B. Boghosian, J. Yepez, P. Coveney, and A. Wagner, *Proc. R. Soc. London, Ser. A* **457**, 717 (2001).
- [16] S. Ansumali and I. V. Karlin, *Phys. Rev. E* **65**, 056312 (2002).
- [17] B. M. Boghosian, P. J. Love, P. V. Coveney, I. V. Karlin, S. Succi, and J. Yepez, *Phys. Rev. E* **68**, 025103(R) (2003).
- [18] Particles have no physical meaning. They represent the smallest computational unit of mass and momentum.
- [19] P. K. Yeung and Y. Zhou, NASA/CR-97-206251 ICASE Report No. 97-64 (1997).